VISUALLY AIDED FORCE CONTROL WITH FUZZY PARAMETER TUNING

by
BERK ÇALLI

Submitted to the graduate School of Engineering and Natural Sciences
in partial fulfillment of
the requirements for the degree of
Master of Science

Sabanci University
August 2008

VISUALLY AIDED FORCE CONTROL WITH
FUZZY PARAMETER TUNING

Berk Çallı

ME, Ms Thesis, 2008

Thesis Supervisor: Assistant Prof. Dr. Kemalettin ERBATUR
Thesis Co-Supervisor: Associate Prof. Dr. Mustafa ÜNEL

Keywords: Visual servoing, Force control, Sensor integration, Fuzzy Logic, Online parameter tuning

ABSTRACT

Vision and force sensors provide rich information which can enable robots to execute complex tasks. The integration of these two types of sensors may prove very useful in many industrial robotic applications, as well as for the robots that operate in environments where humans live. Vision sensors give robots the ability to operate in complex and dynamic environments. With force sensors contacts can be detected, and manipulation tasks can be done without the risk of damaging the workpiece. The integration of vision and force sensing systems equips robots with all these advantages and the abilities of robots can rise dramatically by the integrated use of these sensors. However, this integration is not straightforward. In this thesis, a literature survey about visual servoing and force control is presented firstly. Present integration methods are reported and discussed. A manipulation task is defined as a case study problem. In this problem, a constant magnitude normal force is to be exerted at a fixed point on an object which is free to rotate. Visual servoing and explicit force control techniques are applied next in the task frame formalism to achieve this objective. Disadvantages of the constant parameter controllers are addressed and two solutions in which controller gains are tuned with fuzzy logic systems are presented. The first solution is in the hybrid control category, whereas the second controller is a shared control strategy. These controllers are novel ones; they are the first applications of the fuzzy gain tuning on the integration of vision and force control systems. Experiments are carried out on a two degrees of freedom (DOF) direct drive SCARA type robot and the results obtained with fixed-parameter and fuzzy-tuned control methods are compared. The experimental results show that

using fuzzy gain scheduling for the integration of force and vision systems improves the performance of combined controller and also prevents possible causes of instability.

BULANIK PARAMETRE AYARLAMALI
GÖRÜNTÜ DESTEKLİ KUVVET KONTROLÜ

Berk Çallı

ME, Master Tezi, 2008

Tez Danışmanı: Yrd. Doç. Dr. Kemalettin ERBATUR
İkincil Tez Danışmanı: Doç. Dr. Mustafa ÜNEL

Anahtar Kelimeler: Görüntü Tabanlı Kontrol, Kuvvet Kontrolü, Sensör Birleştirme, Bulanık Mantık, Çevrimiçi Değiştirge Ayarlama

ÖZET

Görüntü ve kuvvet sensörleri, robotlara zengin içerikli bilgi sunarlar. Bu bilgiler robotların karmaşık görevleri başarmalarını sağlar. Bu iki tip sensörün bileştirilmesi sanayide birçok robot uygulamasında ve insanların yaşadıkları ortamlarda çalışan robotlar için gereklidir. Görüntü sensörleri robotlara karmaşık ve dinamik ortamlarda çalışma yetisi kazandırır. Kuvvet sensörleri ile ise, temas sezilebilir ve manipülasyon görevlerinde robot ve manipüle edilen objelerin hasar görmesi önlenebilir. Görüntü ve kuvvet sensorlerinin birleştirilmesi ile ise robot bütün bu avantajlar ile donatılmış olur ve robotun yapabildiği görey sayısı önemli derecede artar. Fakat, bu sensör birleştimesi tek düze bir iş değildir. Bu tezde görüntü tabanlı kontrol ve kuvvet kontrolü konusunda yapılmış bazı araştırmaları sunulmaktadir. Görüntü/kuvvet birleştirmesi konusundaki mevcut çalışmalar irdelenmiştir. Bu methodların denenmesi için bir manipulasyon görevi, durum çalışması olarak tanımlanmıştır. Bu görev, dönme serbestisi olan bir obje üzerindeki sabit bir noktaya, sabit miktarda bir kuvvet uygulamasını içerir. Bu görevi gerçekleştirmek için görüntü tabanlı kontrol ve açık kuvvet tabanlı control teknikleri görev kordinat takımı ile kullanımıştır. Sabit parametre kullanan kontrolörlerin dezavantajları belirtilmiş ve bu dezavantajların üstesinden gelmek için bulanık mantık ayarlaması kullanılan iki çözüm önerilmiştir. İlk çözüm, hibrit control kategorisine girmektedir. İkinci çözüm ise, bir paylaşımlı control stratejisidir. Bu kontrolörler literatürde yenidir; bulanık mantık ile parametre ayarlaması kullanan ilk görüntü ve kuvvet birleştirme çalışmalarıdır. Sabit parametre kullanan kontrolör ve bulanık değiştirgeli kontrolörler, iki serbestlik dereceli, doğrudan işlemeli SCARA tipi robot üzerinde uygulanmış

ve deney sonuçları karşılaştırılmıştır. Deney sonuçları göstermektedir ki, bulanık mantık kullanarak parametre ayarlama yöntemi performası arttırdığı gibi kararsızlığa neden olabilecek robot hareketlerini de önlemektedir.

To my family

ACKNOWLEDGEMENTS

I would like to thank to many people who helped me a lot to overcome the difficulties while working on this thesis.

Firstly, I would like to thank to my thesis supervisor Kemalettin Erbatur. He was always very benevolent, understanding and encouraging to me. He helped me in all my Master Thesis period and made this thesis possible. My thesis co-supervisor Mustafa Ünel is very important for me by giving me a strong background about lots of topics. With the inspiring and joyful discussions with him, I was able to construct some basis ideas of this thesis. I would like to thank to the Volkan Patoğlu for sharing this valuable time and ideas with me. His door was always open, and he inspired me by showing the importance of teaching. Also I would like to thank to Ahmet Onat and Albert Levi for their valuable comments on my thesis.

I would like to thank to Yeşim Hümay Esin for always being with me and supporting me. Without her, not only this thesis but all six years would be much harder and dull.

I would like to thank to my roommate Hakan Kaynar, for always making me cheer no matter the consequences are, my friend Fırat Ant for his guidance and lifetime support, and all my friends in Sabanci University, in Istanbul and in Izmir.

And of course, I would like to express my deepest regards and love to my family. From kilometers away, they make me feel like I am home. Without them, I was completely lost.

VISUALLY AIDED FORCE CONTROL WITH
FUZZY PARAMETER TUNING

TABLE OF CONTENT

LIST OF FIGURES

LIST OF TABLES

LIST OF SYMBOLS

O : Force application point on workpiece.

$\overline{O}$: Force application point on workpiece after movement.

I : Initial position of robot tool tip

P : Pivot point on workpiece

F : Force measurement in y-direction

F^r : Force reference in y-direction

e_F : Force error in task space

S : Selection matrix of hybrid vision/force control

e_{FS} : Force error after selection matrix is applied

F_F^c : Force generated by PI control

K_{p_F} : Proportional gain matrix of PI controller of force control

K_F : Integral gain matrix of PI controller of force control

$K_{p_F x}$: Upper diagonal element of K_{p_F} matrix.

$K_{p_F y}$: Lower diagonal element of K_{p_F} matrix

K_{F^x} : Upper diagonal element of K_F matrix

K_{F^y} : Lower diagonal gain of K_F matrix

R_w^t : Rotation matrix between task frame and world frame

q : Robot joint position vector

$J_R(q)$: Robotic Jacobian

u_F : Torque vector generated by force control

e_V^x : Visual servoing error in x-direction

e_V^y : Visual servoing error in y-direction

e_V : Visual servoing error vector

e_{VS} : Visual servoing error vector after selection matrix is applied

K_V : Visual servoing gain matrix

K_V^x : Upper diagonal element of K_V matrix

K_V^y : Lower diagonal element of K_V matrix

F_V^c : Force vector generated by visual servoing

R_i^t : Rotation matrix between task frame and image frame

J_I : Image jacobian

v^r : Velocity reference generated by visual servoing

p^r : Position reference generated by visual servoing

F_P^c : Force vector generated by cartesian position controler

e_P : Cartesian position error

K_{P_p} : Proportional gain matrix of cartesian position controller

K_{I_p} : Integral gain matrix of cartesian position controller

K_{D_p} : Derivative gain matrix of cartesian position controller

u_P : Torque vector generated by cartesian position controller

u : Torque vector that is applied on robot.

$\mu_{B\,e_{Fy}}$: Membership function variable for big force error in y-direction

$\mu_{S\,e_{Fy}}$: Membership function variable for small force error in y-direction

$\mu_{S\,e_{Vx}}$: Membership function variable for small vision error in x-direction

$\mu_{B\,e_{Vx}}$: Membership function variable for big vision error in x-direction

$\mu_{B\,e_{Vy}}$: Membership function variable for big velocity error in y-direciton

$\mu_{S\,e_{Vy}}$: Membership function variable for small velocity error in y-direciton

$\Delta K_{V^x NS}$: Fuzzy rule base element for negative small change in visual servoing gain in x-direction

$\Delta K_{V^x PS}$: Fuzzy rule base element for positive small change in visual servoing gain in x-direction

$\Delta K_{V^y NB}$: Fuzzy rule base element for negative big change in visual servoing gain in y-Direction

$\Delta K_{V^y PS}$: Fuzzy rule base element for positive small change in visual servoing gain in y-

Direction

$\Delta K_{V^{y}{}_{PB}}$: Fuzzy rule base element for positive big change in visual servoing gain in y-Direction

$\Delta K_{V^{y}{}_{PB}}$: the computation cycle of the digital controller

$\Delta K_{F^{y}}$: Force gain change computed by fuzzy logic

$\Delta K_{V^{x}}$: Visual servoing gain change x-direction computed by fuzzy logic

$\Delta K_{V^{y}}$: Visual servoing gain change y-direction computed by fuzzy logic

α : Task angle (The angle of the workpiece with respect to the world frame)

LIST OF ABBREVIATIONS

FPS : Frame per Second

DOF : Degree of Freedom

PID : Proportional Integral Derivative

PI : Proportional Integral

OpenCV : Open Computer Vision

NS : Negative Small

NB : Negative Big

PS : Positive Small

PB : Positive Big

Chapter 1

1. INTRODUCTION

Using sophisticated sensors on robots enables them to execute more complex tasks. Force and vision sensing abilities are of paramount importance for robotic applications which are beyond the state of art industrial use. Integration of the data from these two different sensors is very promising for manipulation tasks.

In addition to their use in industrial applications, these sensor can be very useful on service robots employed in human living environments, offices hospitals etc. too. These environments are complex and dynamic. This brings the necessity for robots to have vision sensors in order to analyze the surroundings. Many tasks in these environments involve a manipulation phase which requires the sense of touch. It is because of these reasons, that humanoid robots are equipped by vision and force sensors.

Even the applications that can be done using vision or force only can be accomplished with a higher performance when these perceptions are used in combination. An example can be writing on a whiteboard with a robot hand. If this job is done with visual servoing only, since there is no sensory information to indicate whether the pen touches the surface or not, the writing will probably be a dashed line. If a reference inside the wall is given with visual servoing, the robot may break the pen since it does not know how much force it exerts. If the application is done with force control only, the places of the objects and initial position of the robot should be known precisely, which is a very limiting factor.

In this thesis work, a manipulation task is defined as a case study problem. A constant magnitude normal force is to be exerted at a point fixed on an object which is free to rotate. This problem requires the orientation of the object and the location of the point to be detected by the vision system continuously. Two integration methods in which visual servoing and force control gains are tuned by the use of fuzzy logic systems are proposed. These online tuning systems employ force and visual servoing errors as inputs and produce required changes in the controller parameters as outputs. One of our two control systems is of hybrid

nature, whereas the other one is a shared control method. These controllers are novel ones of fuzzy logic application on vision/force integration.

Chapter 2

2. LITERATURE SURVEY

Although the base of this thesis is about integration of force control and visual servoing, surveys about the members of this integration can be very useful and give ideas for some future work. Thus, this chapter begins with the main algorithms about visual servoing and force control. After that, vision/force integration methods are discussed. A survey about fuzzy logic, on which the integration strategies in this thesis are based, is presented. At the end of this chapter, vision/force integration methods in literature has been discussed.

2.1 Visual Servoing

In 70's and 80's, most of the work on vision based control is based on static look and move approach. Static look and move approach is an offline approach which is made up of taking an image at target position and at initial position, and applying control to be able to reach the target position. An example of static look and move approach is in [1]. In the same era there are also works that aim to generate trajectory for robots based on image features in an offline manner [2].

Visual servoing literature becomes intense in 90's as real-time image processing became possible. In this decade, these developments, by the means of image acquiring speed and resolution, enable visual servoing algorithms to be used online.

A classification of visual servoing algorithms that are developed after 90's is given in [3] concerning control structure and definition of the error signal. Depending on the control structure, if visual servoing is used along with an inner control loop which uses joint encoder information, than this structure is called dynamic look-and-move. In this kind of visual servoing, visual servoing rule generates references to an inner encoder based position

controller. On the other hand if this internal loop is not used, then this kind of visual servoing is called direct visual servoing. In this kind of servoing visual controller directly generates torques to the actuators.

Concerning direct visual servoing and dynamic look and move approaches, Peter Corke's Ph.D. work, [4], can be considered as a milestone. Corke addresses the difficulties as visual servoing is used in a direct manner. He indicates that low frame per second (fps) rates of the cameras and nonlinear dynamics of the robots creates stability problems in visual servoing application. Since camera sampling rate is much lower than the sampling rate of the encoder based position controller, if the visual servoing is used alone, the bandwidth of the system drops dramatically. Also, leaving vision alone to overcome the difficulties of the dynamics of the robots gives worse results in most of the cases than treating the dynamics with an inner position controller. Thus, to enhance stability in these applications, he suggests using dynamic look and move approaches.

Depending on the error signal, visual servoing systems can be grouped as imaged based visual servoing, position based visual servoing and hybrid approaches. If the error signal is defined between the desired image feature locations and current image feature locations, then this type of servoing is called image based visual servoing [5,6]. If image features are used to reconstruct the pose (translation and orientation) of the workpiece, and error is defined between desired and current workpiece pose, then this type of servoing is called position based visual servoing [7,8]. Unlike image based visual servoing, position based visual servoing needs calibrated camera and geometric model of the workpiece as a priory information. The performance of the position based visual servoing is very much dependent on these data. 2 and ½ D visual servoing [9], which is a hybrid approach, involves properties from both image based visual servoing and position based visual servoing.

There are also switching approaches as in [10]. These approaches switch among different kind of visual servoing systems by a help of supervisory system. As it is seen in [10], this kind of approaches combines the advantages of the visual servoing algorithms and may be able to avoid the disadvantages.

Also many nonlinear control algorithms have been adapted to visual servoing. There are visual servoing algorithms that are robust to calibration errors [11, 12]. In addition to that there are adaptive visual servoing methods that estimate camera calibration parameters as in [13,14]. Moreover, there are learning based visual servoing algorithms as in [15] which can be used for periodic tasks.

2.2 Force Control

Force control is a widely studied topic in last three decades, and various force control techniques have been developed. [16] gives a survey on force control as well as a classification of force control techniques. Among these techniques stiffness control, impedance control, admittance control, hybrid control, explicit force control, implicit force control are given as fundamental types. As advanced types, adaptive force control, robust force control, and learning force control can be listed.

In many industrial applications, a contact with the workpiece is needed but the amount and direction of the force exerted are not important. Passive compliance method is widely used (which is also called passive stiffness control). In this method, a compliance mechanism (springs and dampers) is attached to the end effector. In active stiffness control, the stiffness of the close loop systems can be designed. An example of stiffness control can be found [17].

In impedance control, the mechanical impedance of the robot, which is defined as $\frac{F}{V}$ where F is the force exerted and V is the velocity of the robot, can be designed while tracking a motion trajectory at the same time. Hogan [18] has introduced the impedance control concept in robotics. This idea is used also in sensor fusion methods and with hybrid approaches.

Admittance of a robot is defined as the inverse of the impedance, $\frac{V}{F}$. The purpose of the admittance control is to alter the mechanical admittance of the robots in a similar manner with impedance control. The examples of admittance control are [19,20]. The difference between admittance and impedance control is that admittance control gives more importance to force trajectory tracking than the motion tracking, and impedance control is vice versa. Thus admittance control is more suitable for high impedance manipulators (manipulators with high gear ratios, heavy structure), and impedance control is suitable for low impedance machines (manipulators with low gear ratios and light structure).

Hybrid position/force control is first introduced in [21]. This idea divides the workspace into orthogonal directions and applies pure force control along some directions and pure position control along some other directions. Which control to be used is chosen by the selection matrix idea. Other examples of hybrid position/force control are [22-24].

Among the hybrid force control techniques there is also a hybrid impedance control technique. This technique enables the control engineer to design impedance of the device while using the hybrid control architecture. This kind of controller is used in [25].

One of the simplest force control algorithms is explicit force control. It uses the difference between measured force and reference force to generate control signal. Mostly this error signal is used in a PID control. However, although the structure of this control algorithm is very simple, designing a stable explicit force controller is not an easy task. [26] examines the factors which affect the stability of these kind of controllers with root-locus plots. It detects that flexibility between force sensor and robot arm creates a bandwidth limitation. Also, [27] investigates this kind of control too. It test various controller structures within the explicit force control framework and specifies PI controller as the most suitable one.

Using the above mentioned control methods as basis, more force controllers are designed for different reasons. If there are unknown robot or environment parameters, an adaptive force control method can be designed to estimate these parameters ([28],[29]). If parameters are known up to a certain error bound, then robust force control techniques can be used ([30]). If the task is periodic, a learning algorithm can be used to improve the performance of the control. An example of usage of learning control along with hybrid position force control can be found in [31, 32].

2.3 Integrated Vision/Force systems:

Before giving a survey about vision/force integration related literature, a classification and explanation of multisensory integration/fusion may be useful. [33] gives basic sensor integration/fusion methods and underlines the differences between sensor fusion and integration. Sensor fusion is the representation of the different sensory information in one mathematical format. On the other hand, sensor integration stands for a more general combination of sensory information, using intelligent combination algorithms etc, to be able to accomplish a certain task. This section includes both integration and fusion methods on vision/force combination.

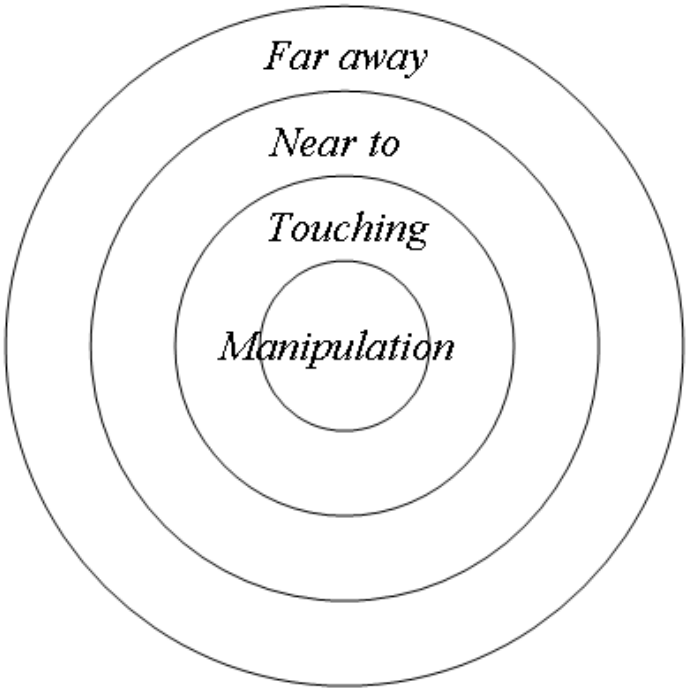

Figure 2.1 Hierarchical Phase Template for sensor integration techniques

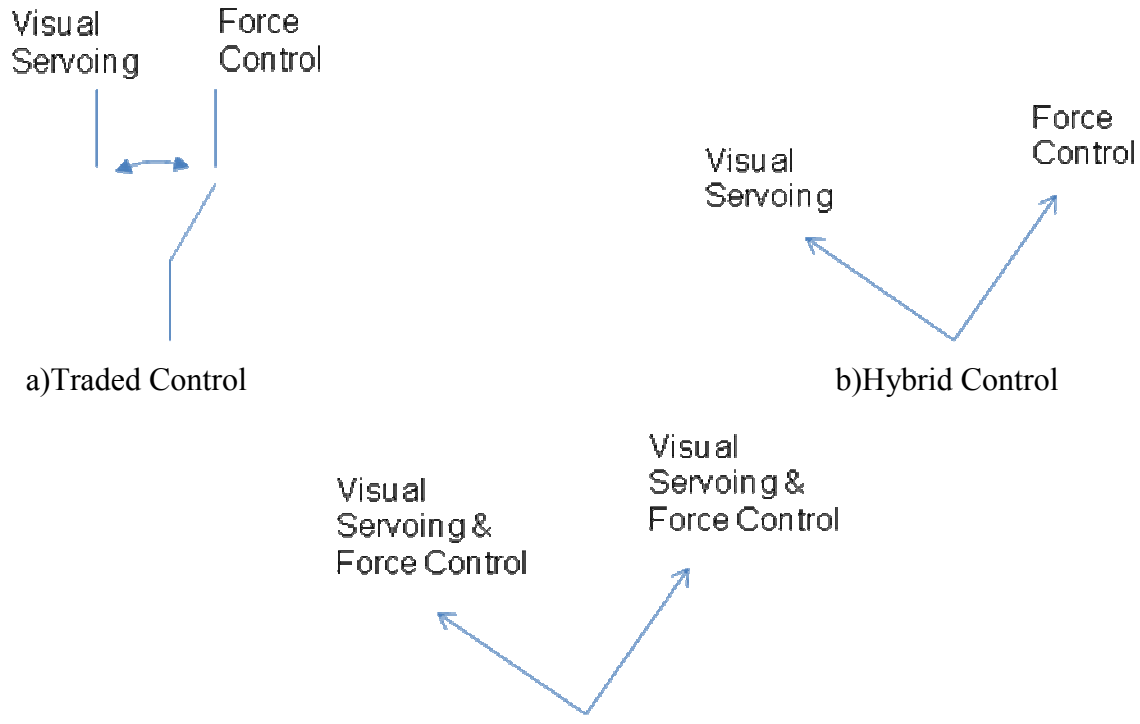

Figure 2.2 Vision/Force Integration Techniques

The methods of integration of force control and visual servoing can be categorized as traded control, hybrid control and shared control [34]. Traded approach means switching between force control and visual servoing for a given direction. In hybrid control, using vision and force are used in separate directions. Shared control uses force and visual servoing in the same direction simultaneously. Figure 2.2 summarizes these methods. Each method has different advantages and drawbacks. Traded control can prevent hard impacts on the workpiece. By this way a possible destabilization effect can be prevented too. Hybrid control is easily applicable in some cases, but vision and force control are decoupled in this type of control. Therefore, a force reference in visual servoing direction or a visual reference in the force control direction can not be applied. This limits the use of hybrid force/vision control. Shared control does not have this kind of disadvantage, and it is regarded as highest level of integration in [35]. However, according to [34], this control has the following drawback: Force sensors measure all forces including inertial, gravitational and tactile forces. These forces create undesired force control outputs which destabilizes the system. This problem can be solved either by compensation or a robust
control system. All these kind of integration algorithms are implemented and the results are discussed in [34].

There are also impedance based combinations of visual servoing and force control achieved by Malis [36]. This approach is made up of a visual servoing control system and a position based impedance controller. Here, vision system provides a reference trajectory to the position based impedance controller.

An approach which is a combination of traded, hybrid and shared control strategies in a task frame formalism is present in [35]. In this methodology, the force and visual servoing directions are decoupled as in hybrid case, but sensors aid each other by generating feedforward control outputs.

2.4 Fuzzy Logic

Fuzzy logic is proposed by Lotfi Zadeh in 1965 for data processing applications [37]. Zadeh defines fuzzy logic as “computing with words”, and states that fuzzy logic is necessary if the rule to be defined is so imprecise that it can not be expressed numerically [38]. In [38]

he also states that the systems which the fuzzy logic is applied on should have a tolerance of imprecision.

The applications of fuzzy logic on control theory start to appear in 70's as the computational capability of the computers are improved. These control methodologies provide an extensive freedom for control designers to exploit their understanding of the problem, to deal with problems of vagueness, uncertainty or imprecision and learn from experience. Fuzzy control and adaptation systems, as tools against the problems of uncertainty and vagueness, incorporate human experience into the task of controlling a plant. When employed in robotic trajectory control, they mainly play one of two roles in the controller architecture. One of them is to compute the control signal by fuzzy rules. The other one is to tune, adapt or schedule the parameters of control mechanisms to accomplish better performance in face of uncertainties and different operating conditions. The former method is called direct approach whereas the latter is called indirect approach. Examples of direct and indirect approaches in control parameter tuning can be found in [39] and [40] respectively.

Chapter 3

3. PROBLEM DEFINITION

Fig. 3.1 shows the scenario of the manipulation task. From the upper left sketch in this figure to the bottom right one, the task description goes through following phases:

In the first phase, robot tool tip starts far away from the workpiece, like the point I in Fig. 3.1 a). The aim of the robot is to apply a constant magnitude force on the point O normal to the edge of the workpiece where O is located. This is a planar manipulation task. To accomplish this aim, robot should approach to point O perpendicularly. First the robot should be brought on the y-axis as shown in Fig. 3.1 a).

As the tool tip reaches the y-axis, robot should approach to the workpiece by following the y-axis as shown in Fig. 3.1 b). When a contact with the workpiece is sensed, desired constant force should be exerted on the workpiece in normal direction as shown in Fig. 3.1 2 c). The robot is also expected to continue exerting the force reference, and should reestablish the contact in the case of a contact loss. The workpiece is free to rotate about the pivot point P. In the experiments, the workpiece is rotated intentionally about this point in order to create contact losses. This phase is shown in Fig. 3.1 d). This is the most demanding phase for a control system, because application of forces on points on the edge of the workpiece other than the location indicated by the black point in Fig. 3.1 is undesired. The interaction of the robot tool tip with the workpiece can be in many different ways while it moves from point O to point $\overline{O}$ in Fig. 3.1 d). However, our target in control synthesis is to achieve an interaction which fulfills demands described above.

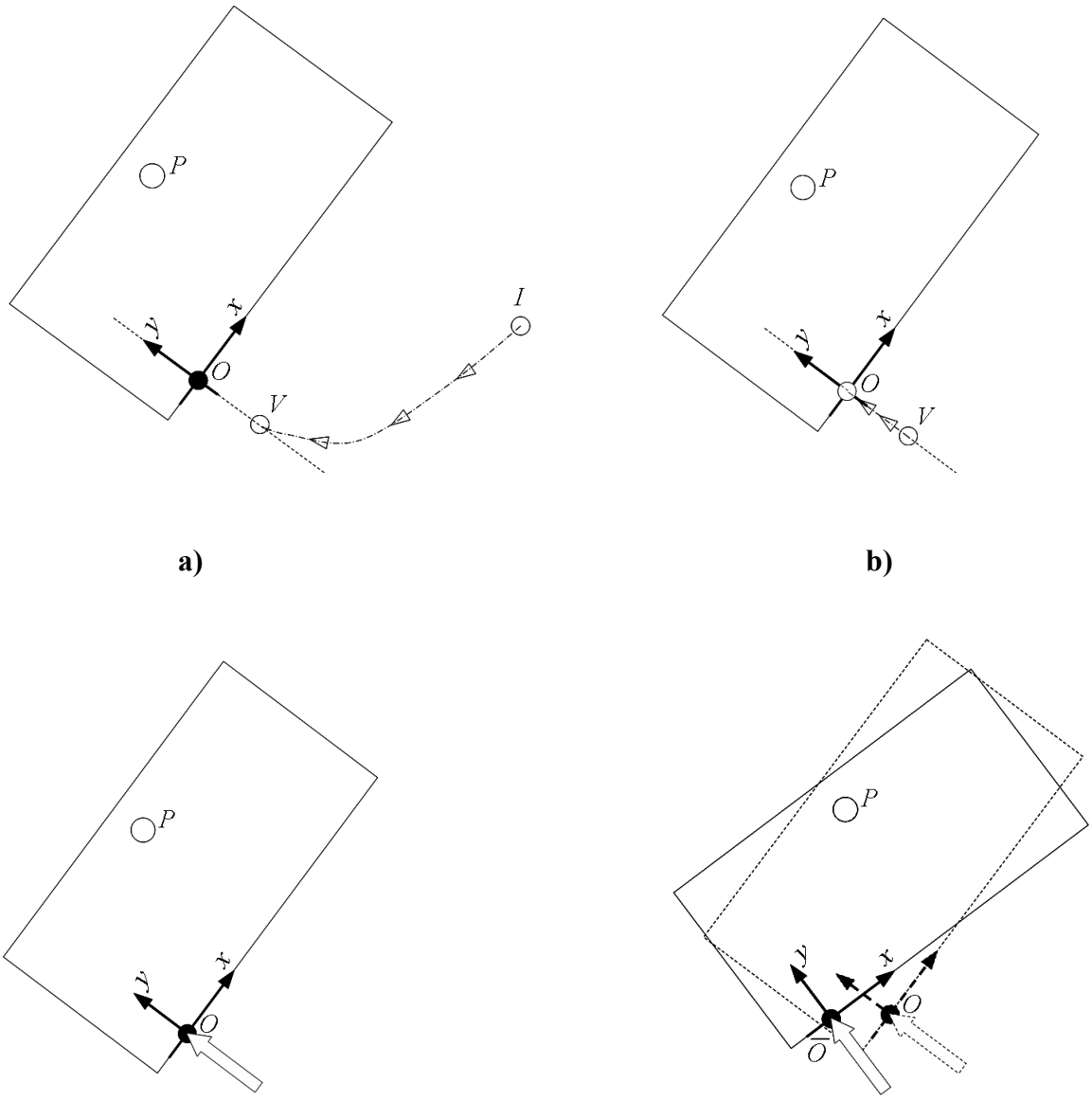

Fig. 3.1 The manipulation scenario.

Chapter 4

4. FIXED PARAMETER HYBRID VISUAL/FORCE CONTROL

Firstly, we design a fixed parameter controller for the problem definition stated in the previous section. This controller is based on the task frame approach. The origin of the task frame is attached on the contact point of the workpiece. Hybrid control is applied with a visual servoing component in the direction tangent to the straight edge of the workpiece and force control component normal to this straight edge. Since a force normal to its contour is to be applied on the workpiece, the orientation of the task frame can be identified with the slope of the edge detected on the workpiece by vision system. The x, y-axis and origin O shown in Fig. 3.1 describe the task frame. For force control, an explicit force controller in PI structure is used. Another natural choice for force controller is impedance control. However, with several experiments it is seen that, the robot that is used as a test bed in this thesis is not suitable for impedance control, because it has a high impedance. As it is mentioned in literature survey chapter of the thesis, for high impedance manipulators admittance control is much more suitable. However, the aim of this thesis is to demonstrate the performance of fuzzy parameter tuning in vision/force integration, and using simpler explicit force control is more advantageous in that sense, because has only one dominant gain parameter to be tuned.

The force error is defined as the difference between the task space force reference F^r and the measured interaction force F:

$$e_F = (F^r - F) \tag{4.1}$$

The "selected force error" is then obtained by

$$e_{FS} = S(F^r - F) \tag{4.2}$$

where the diagonal matrix S is called the selection matrix. The entries of this matrix specify the force controlled task space directions. If the i^{th} direction is a force controlled one, then the i^{th} diagonal term s_{ii} of S is equal to 1 and it is equal to 0 otherwise. The force control law is expressed as

$$F_F^c = K_{p_F} e_{FS} + K_F \int e_{FS} dt \tag{4.3}$$

In (4.2), F_F^c stands for the Cartesian control force defined in the task space. K_{p_F} is the diagonal proportional force control gain matrix and K_F is the diagonal integral gain matrix:

$$K_{p_F} = \begin{bmatrix} K_{p_F x} & 0 \\ 0 & K_{p_F y} \end{bmatrix}, \qquad K_F = \begin{bmatrix} K_{F^x} & 0 \\ 0 & K_{F^y} \end{bmatrix}. \tag{4.4}$$

The control F_F^c is then transformed into robot joint torques by using the robot Jacobian J_R as,

$$u_F = J_R^T(q) R_w^t F_F^c \tag{4.5}$$

where q is the vector of joint positions and R_w^t is the rotation matrix between the task frame and the world frame attached to the base link of the manipulator. u_F stands for the force control component in the joint control torques. $()^T$ signifies the transpose of a matrix.

The vision based position control adopted in this thesis is in the so-called "dynamic look-and-move" control category. In dynamic look-and-move approach, visual servoing generates position references for an inner position control loop based on joint encoder feedback.

Task space errors e_V^x and e_V^y (measured in pixels) for visual servoing are defined in Figure 4.1. Augmenting them together, the task space position error e_V is obtained:

$$e_V = \begin{bmatrix} e_V^x \\ e_V^y \end{bmatrix} \tag{4.6}$$

Its "selected" version is obtained by

$$e_{VS} = (I - S)e_V \tag{4.7}$$

where I stands for the identity matrix. With (4.5) and with the definition of the selection matrix above the position errors in the force controlled directions are ignored. The visual servoing rule in the image space is defined as,

$$F_V^c = K_V e_{VS} \tag{4.8}$$

In (6), F_V^c is the task space control force vector generated by visual servoing and K_V is a gain matrix in diagonal form

$$K_V = \begin{bmatrix} K_V^x & 0 \\ 0 & K_V^y \end{bmatrix}. \tag{4.9}$$

In this thesis, F_V^c is not used as a Cartesian control force to be converted to joint torques via a Jacobian-Transpose relation. Rather, this vector is used to generate world frame Cartesian tool tip position references. F_V^c is regarded as the task space velocity demand for the visual servoing task. It is expressed firstly in the image frame coordinates by pre-multiplying it by the rotation matrix relating the task frame coordinates to the image frame coordinates. Then, it is expressed in world frame by the multiplication by the rotation matrix that is defined between world frame and image frame, and the image Jacobian is used to obtain the velocity demand as expressed in world frame coordinates and units:

$$v^r = R_w^i R_i^t F_V^c \tag{4.10}$$

Here v is the task space velocity demand in m/sec. J_I is the image Jacobian which includes camera intrinsic parameters. The position reference p^r in the world frame is obtained by integrating this velocity demand as in the following equation.

$$p^r = \int v^r dt \tag{4.11}$$

Let p be the actual Cartesian position of the robot tool. (p is obtained through joint encoder readings and forward kinematics with the position control loop sampling rate, which is higher than the camera sampling rate.) Defining e_P, the Cartesian position error expressed in the world frame, by $e_P = p^r - p$, a PID position controller is used to generate a Cartesian control force for the robot tool as below.

$$F_P^c = K_{P_p} e_P + K_{I_p} \int e_P dt + K_{D_p} \dot{e}_P \tag{4.12}$$

This force is reflected to joint control torques by the use of the manipulator Jacobian:

$$u_P = J_R^T F_P^c \tag{4.13}$$

As in the case of u_F, u_P is a component in the joint control torque vector. The joint control vector u is finally computed as

$$u = u_F + u_P \tag{4.14}$$

As mentioned in chapter 3, the task in this thesis is the application of a normal force to a workpiece. We divided this task into two phases: i) Reaching phase and ii) manipulation phase. In the reaching phase, the tool tip of the robot is brought near the force application point using visual servoing in task frame. In this phase the both of the task frame directions are visually controlled. Therefore, the selection matrix S is given by

$$S = \begin{bmatrix} 0 & 0 \\ 0 & 0 \end{bmatrix} \tag{4.15}$$

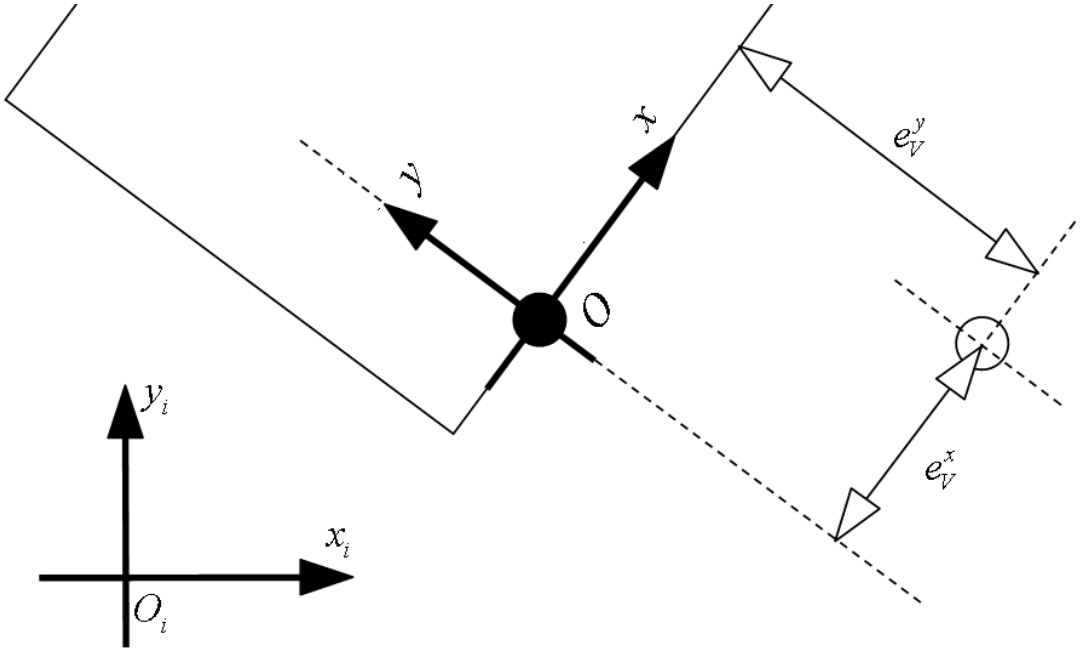

Fig. 4.1 Visual servoing errors.

In the reaching phase, the visual servoing gain in x direction is specified higher than the visual servoing gain in y direction, in order to quickly bring the tool tip to the line of concern (task frame y-axis). After intersecting it, the robot tool moves along with the y axis of the task frame and touches the surface of the workpiece. The contact is sensed by the force sensor by measuring the force in y direction in task space. A force threshold is employed for the contact detection. With the contact, second phase begins.

In the second phase hybrid position/force control guided by visual servoing is applied. Along the y direction force control is applied, and visual servoing is implemented along the x direction. This corresponds to the following selection matrix.

$$S = \begin{bmatrix} 0 & 0 \\ 0 & 1 \end{bmatrix} \tag{4.16}$$

Since the problem definition in chapter 3 involves a free-to-rotate workpiece, after the reaching phase, the object is manually rotated around the pivot point P shown in Fig. 2. In this phase, even if there appears a position error in x-direction, the controller continues applying force. This results with the application of force on undesired points of the workpiece. High values for visual servoing gains may be suggested as a solution of this problem. With high control gains, visual servoing can push the x-direction position error

quickly to zero. However, using high gain values can result with overshoot and oscillations. As another problem, if force control continues when the contact is lost, some hard impacts are inevitable. Though hard impacts can be avoided by using very low force control gains, low gains result in a very slow force control reaction. All these phenomenon are also observed in the experiments.

It can also be argued that a solution to the problems above can be obtained by switching to the pure visual servoing case (to reaching phase) whenever the contact with the workpiece is lost. However, in many cases, detecting the loss of contact is problematic because both vision and force sensors are noise prone. The relatively low resolution of the vision system worsens the problem of contact loss detection too.

The performance of this approach is further considered in the experimental results chapter.

In order to overcome the disadvantages of the method discussed above, online fuzzy tuning methods are devised for both visual servoing and force control gains. These fuzzy tuning schemes are presented in the next chapter.

Chapter 5

5. HYBRID CONTROL WITH FUZZY PARAMETER TUNING

The dominant control gain in force control is K_F. According to [28] an effective use of the explicit force control scheme can be obtained by selecting a K_F value much larger than K_{p_F} in [28]. Therefore the gain K_F is chosen for tuning the force controller by fuzzy rules. In the vision control law (4.6) the only gain is K_V, and this gain is tuned by a fuzzy system.

The main principles of the tuning are as follows.

i. If the position error is big and force error is small, then this means that the robot is applying the reference force to an undesired point. The robot should be brought on the line of concern (task space y-axis) without applying too much force on the workpiece. To accomplish this force gain should be decreased, and vision gain should be increased.
ii. If the position error is small and force error is big, this means the robot is at the right position, but force control gain is too low that the desired force value has not reached yet. To overcome this, force control gain should be increased. And also to avoid fast movements in tangential direction, motion in visually guided direction should be softened.
iii. If both position and force error are big, this means the workpiece went through a large motion. In this case, the force gain should be decreased rapidly and visual servoing should be increased.
iv. If both of the position error and force error are small, then there is no need to change the control gains.

These four principles can be implemented by two independently running fuzzy tuning systems for the two controller gains mentioned above. The rule bases for these fuzzy systems

for K_F and K_V are summarized in Tables 5.1 and 5.2, respectively. Note that the tuning is carried out for the "active" entries of the gain matrices corresponding to the force and vision controlled directions chosen by the selection matrix S. Fig. 5.1 shows the membership functions for the input variables of rule bases in Tables 5.1 and 5.2. . In the tables the subscript "NB" stands for negative big, "NS" is negative small and "PS" is positive small. The numerical values for rule strengths ΔK_{F^yPS}, ΔK_{F^yNB}, ΔK_{F^yNS}, ΔK_{V^xNS}, ΔK_{V^xPS} and ΔK_{V^xPS} the corner positions e_{F^yS}, e_{F^yB}, e_{V^xS} and e_{V^yS} of the trapezoidal membership functions in Fig. 5.1 are tabulated in the experimental results chapter. "Δ" in the notation for the rule strengths signifies that, instead of computing the control gains directly, incremental changes in the control gains are computed by the fuzzy systems. The defuzzification rules are,

$$\Delta K_{F^y} = \frac{\mu_{B\mathrm{e}_{\mathrm{F^y}}}\mu_{S e_{V^x}}\Delta K_{F^yPS} + \mu_{B\mathrm{e}_{\mathrm{F^y}}}\mu_{B e_{V^x}}\Delta K_{F^yNB} + \mu_{S\mathrm{e}_{\mathrm{F^y}}}\mu_{B e_{V^x}}\Delta K_{F^yNS}}{\mu_{B\mathrm{e}_{\mathrm{F^y}}}\mu_{S e_{V^x}} + \mu_{B\mathrm{e}_{\mathrm{F^y}}}\mu_{B e_{V^x}} + \mu_{S\mathrm{e}_{\mathrm{F^y}}}\mu_{S e_{V^x}} + \mu_{S\mathrm{e}_{\mathrm{F^y}}}\mu_{B e_{V^x}}} \tag{5.1}$$

$$\Delta K_{V^x} = \frac{\mu_{B\mathrm{e}_{\mathrm{F^y}}}\mu_{S e_{V^x}}\Delta K_{V^xNS} + \mu_{B\mathrm{e}_{\mathrm{F^y}}}\mu_{B e_{V^x}}\Delta K_{V^xPS} + \mu_{S\mathrm{e}_{\mathrm{F^y}}}\mu_{B e_{V^x}}\Delta K_{V^xPS}}{\mu_{B\mathrm{e}_{\mathrm{F^y}}}\mu_{S e_{V^x}} + \mu_{B\mathrm{e}_{\mathrm{F^y}}}\mu_{B e_{V^x}} + \mu_{S\mathrm{e}_{\mathrm{F^y}}}\mu_{S e_{V^x}} + \mu_{S\mathrm{e}_{\mathrm{F^y}}}\mu_{B e_{V^x}}} \tag{5.2}$$

These functions characterize fuzzy systems with singleton fuzzification, product inference rule and center average defuzzifiers. Finally, K_{F^y} and K_{V^x} are obtained by

$$K_{F^y}(k+1) = K_{F^y}(k) + \Delta K_{F^y}(k) \tag{5.3}$$

and

$$K_{V^x}(k+1) = K_{V^x}(k) + \Delta K_{V^x}(k) \tag{5.4}$$

respectively. In (5.3) and (5.4), k is the computation cycle of the digital controller. If, by the fuzzy logic, the force control or visual servoing gain is tuned to the lowest possible value, which is set by the designer, then that control is turned off.

As also discussed in the experimental results chapter, this online tuning method is successful in avoiding the undesired sheer (tangential) forces on the workpiece. It brings the tool tip of the robot with the point of concern on the y-axis. However, when the error in x-direction is

reduced via visual servoing, according to the fuzzy rules, force control gain begins to rise. If there is a nonzero position error in y-direction in that instance, this fuzzy tuned control system cannot avoid a hard impact.

Table 5.1 The Fuzzy Rule Base for Tuning the y-Direction Force Control Gain

e_{F^y} \ e_{V^x}	Small e_{V^x}	Big e_{V^x}
Big e_{F^y}	$\Delta K_{F^y PS}$	$\Delta K_{F^y NB}$
Small e_{F^y}	0	$\Delta K_{F^y NS}$

Table 5.2 The Fuzzy Rule Base for Tuning the x-Direction Visual Servoing Gain

e_{F^y} \ e_{V^x}	Small e_{V^x}	Big e_{V^x}
Big e_{F^y}	$\Delta K_{V^x NS}$	$\Delta K_{V^x PS}$
Small e_{F^y}	0	$\Delta K_{V^x PS}$

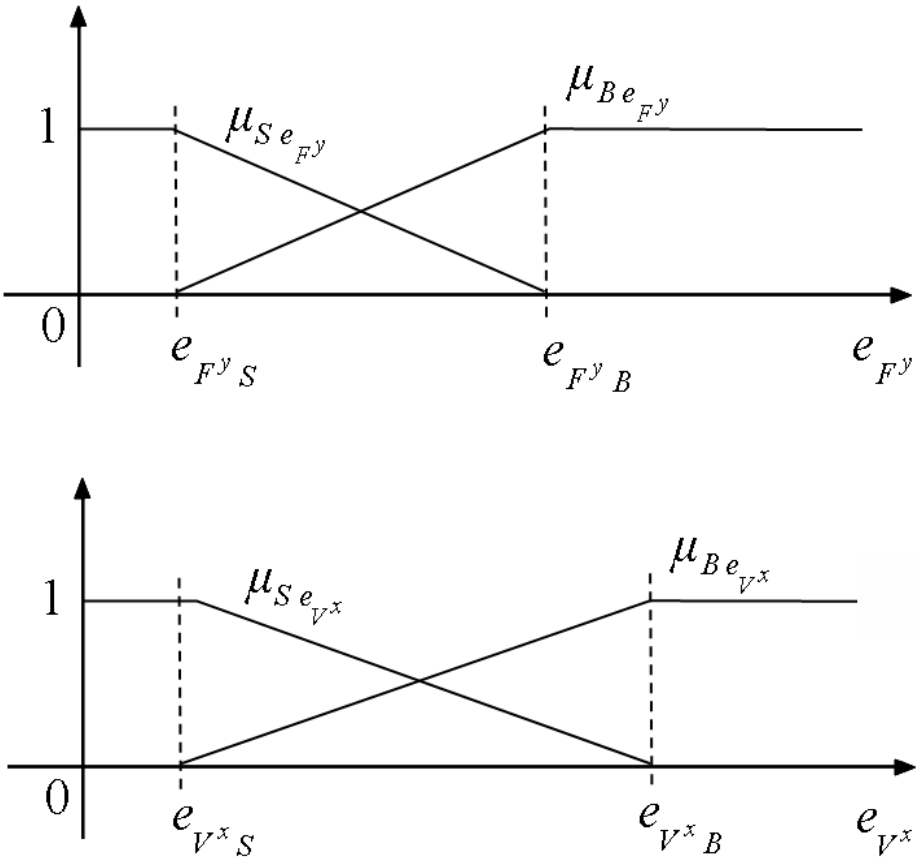

Figure 5.1 Membership functions used in the fuzzy inference of the first fuzzy tuning system (Hybrid control architecture).

To solve this problem, we propose a third fuzzy gain tuning system which is discussed in the next chapter. This system tunes the visual servoing gain in y -direction.

Chapter 6

6. SHARED CONTROL WITH FUZZY PARAMETER TUNING

In the two approaches described in Chapters 4 and 5, the visual servoing gain K_V^y does not enter control computations after the first contact with the workpiece because of the selection matrix choice given in (4.16) for the manipulation phase. The hard impact problem mentioned in Chapter 5, however, can be tackled by modifying the selection matrix and continuing with visual servoing in the y-direction in the manipulation phase too. In this chapter we use a control action selection mechanism which employs two selection matrices in the manipulation phase to replace the force and vision error computation equations in (4.2) and (4.7) by

$$e_{FS} = S_1(F^r - F) \tag{6.1}$$

and

$$e_{VS} = S_2 e_V \tag{6.2}$$

respectively. In the last two equations, S_1 and S_2 are given by

$$S_1 = \begin{bmatrix} 0 & 0 \\ 0 & 1 \end{bmatrix} \text{ and } S_2 = \begin{bmatrix} 1 & 0 \\ 0 & 1 \end{bmatrix} \tag{6.3}$$

The control action selection approach in (6.1-6.3) makes the y-direction a shared control direction. This approach not only closes the distance between workpiece and robot tool tip (and thus avoids a hard impact), but also, with our fuzzy tuning method if the visual servoing reference is given slightly into workpiece, it acts like a feedforward action for force control. This feedforward action makes force control converge faster to the force reference.

The fuzzy rule base for visual servoing in the (originally force controlled) y-direction is designed using the following principles.

i. If both vision and force errors are big, this means the tool tip is far away from the workpiece, and visual servoing gain in y-direction should be raised to decrease this error.
ii. If vision error is small and force error is large, it may be good that visual servoing contributes on force exertion task. However, this contribution should slowly fadeout and should leave its place to force control. Thus, in this phase, visual servoing gain should be decreased slowly.
iii. If both force and vision errors are small. This means that if there is still a contribution from visual servoing on exerting force in y-direction, this effect should be quickly reduced in order not to exceed the force reference. Therefore, a big decrease in visual servoing gain is necessary.

The table 6.1 presents the rule used for the fuzzy tuning of gain K_V^y. It is interpreted in a way similar to the rule bases in the previous chapter. Note that, a new input variable, the position error e_{V^y} is employed for this tuning system too. (6.2) and (6.3) below compute K_V^y in a way similar to the gain computations in the previous chapter too.

Table 6.1 The Fuzzy Rule Base for Tuning the y -Direction Visual Servoing Gain

e_{Fy} \ e_{Vy}	Small e_{Vy}	Big e_{Vy}
Big e_{Fy}	0	ΔK_{VyPB}
Small e_{Fy}	ΔK_{VyNB}	ΔK_{VyPS}

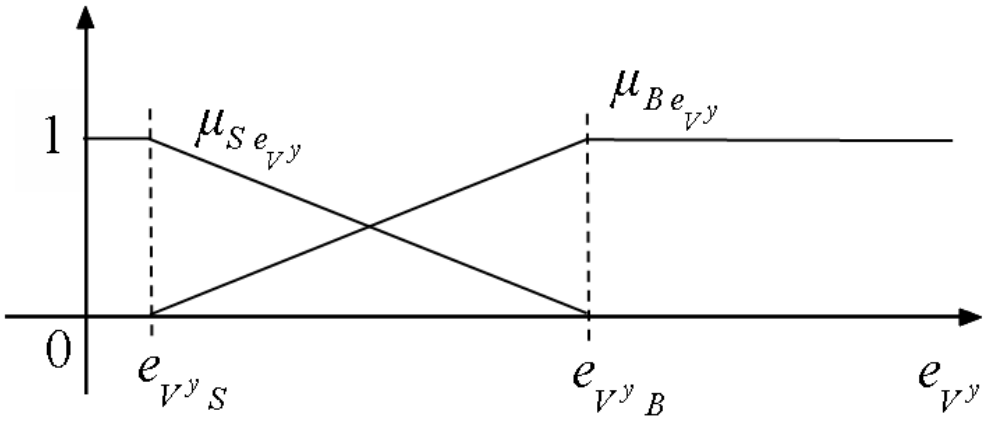

Figure 6.1 Membership function of the fuzzy logic that tunes the Visual servoing gain in y direction

The defuzzification rule is given in Eqn. (6.4)

$$\Delta K_{Vy} = \frac{\mu_{Be_{Fy}}\mu_{Be_{Vy}}\Delta K_{Vy_{PB}} + \mu_{Se_{Fy}}\mu_{Se_{Vy}}\Delta K_{VyNB} + \mu_{Se_{Fy}}\mu_{Be_{Vy}}\Delta K_{VyPS}}{\mu_{Be_{Fy}}\mu_{Be_{Vy}} + \mu_{Se_{Fy}}\mu_{Se_{Vy}} + \mu_{Se_{Fy}}\mu_{Se_{Vy}} + \mu_{Se_{Fy}}\mu_{Be_{Vy}}}. \quad (6.4)$$

And the update rule is,

$$K_{V^y}(k+1) = K_{V^y}(k) + \Delta K_{V^y}(k) \tag{6.5}$$

The next chapter presents experimental results obtained with this method and the methods discussed in Chapters 4 and 5.

Chapter 7

7. EXPERIMENTAL RESULTS

In this chapter, the experimental setup including the robotic system and sensory equipment is introduced. The methodologies that are used in implementation steps are discussed. Finally, experimental results are given and discussed.

7.1 Robotic system

A two-DOF direct drive manipulator built at Sabanci University Robotics Laboratory is shown in Fig. 7.1, and also in Fig. 7.2 in the experiment scenario touching the workpiece with its tool tip. This manipulator is used as the test bed in the experimental studies. A dSPACE 1102 DSP-based system is used to control the arm. The user interface software runs on a PC. C language servo routines are compiled in this environment and downloaded to the DSP. The Yokogawa Dynaserv direct drive motors used at base and elbow joints provide position measurement signals with a resolution of 1024000 pulses/rev. The base motor torque capacity is 200 Nm and that of the elbow motor is 40 Nm.

The various link length, mass and inertia parameters of the robot are tabulated in Table 7.1 as a reference to describe the nonlinearities, coupling and friction effects involved in the experiments. Link inertia parameters and center of mass locations are computed from the CAD models of the links. Link lengths and joint to center of mass distances are indicated in Fig. 7.3. Link inertia values I_1 and I_2 are computed about axes which are perpendicular to the sketch plane and which run through the center of mass points c_1 and c_2 shown in this figure. Rotor inertia values J_1 and J_2 are taken from the manufacturer's documentation. Friction parameters, especially Coulomb friction, however, are difficult to model. Still, rough

estimates of viscous friction coefficients and Coulomb friction terms obtained experimentally using force sensors are listed in Table 7.1 too.

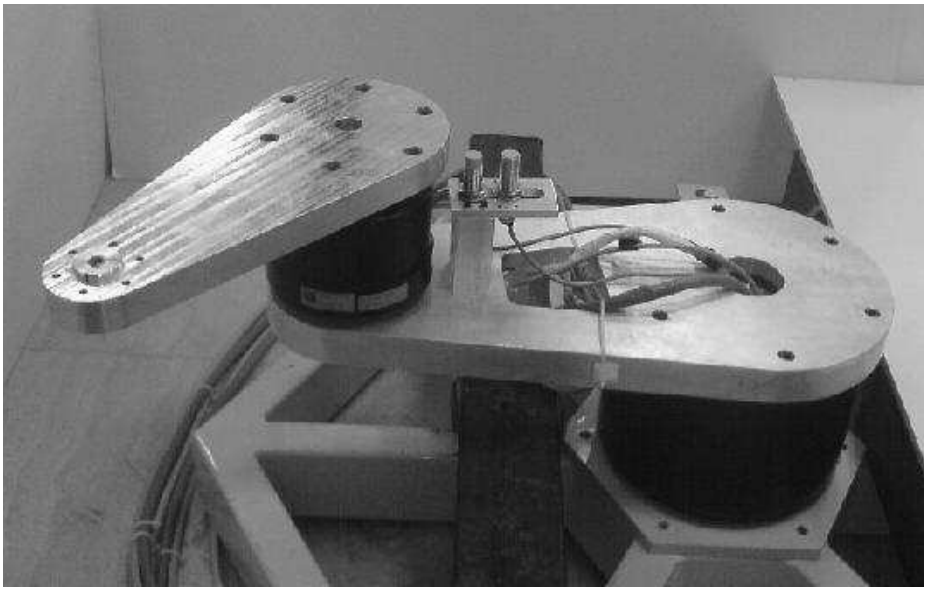

Figure 7.1 Direct Drive Scara Robot

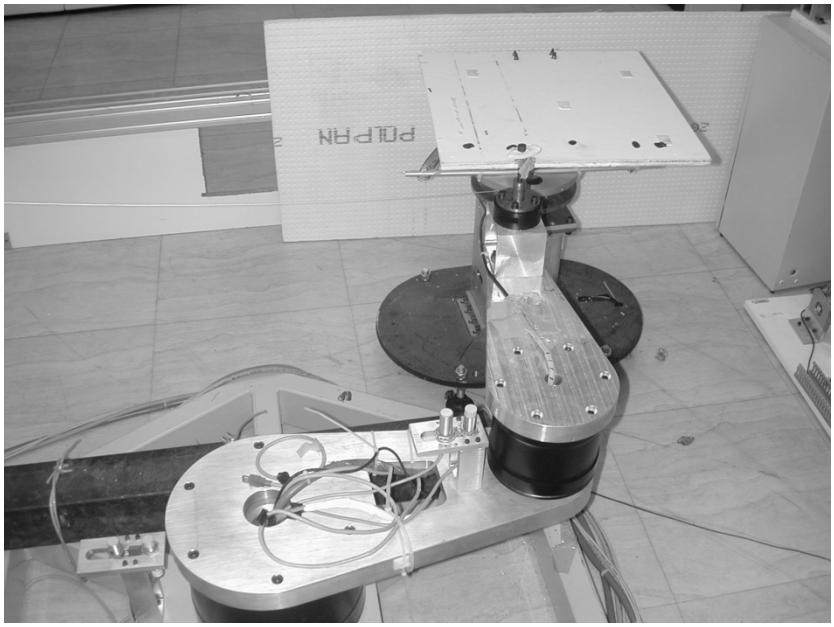

Figure 7.2 The experimental setup. This scene is overlooked by the camera which is fixed at a location above the workpiece. The robot is equipped by a 6-axis force sensor at its tool tip.

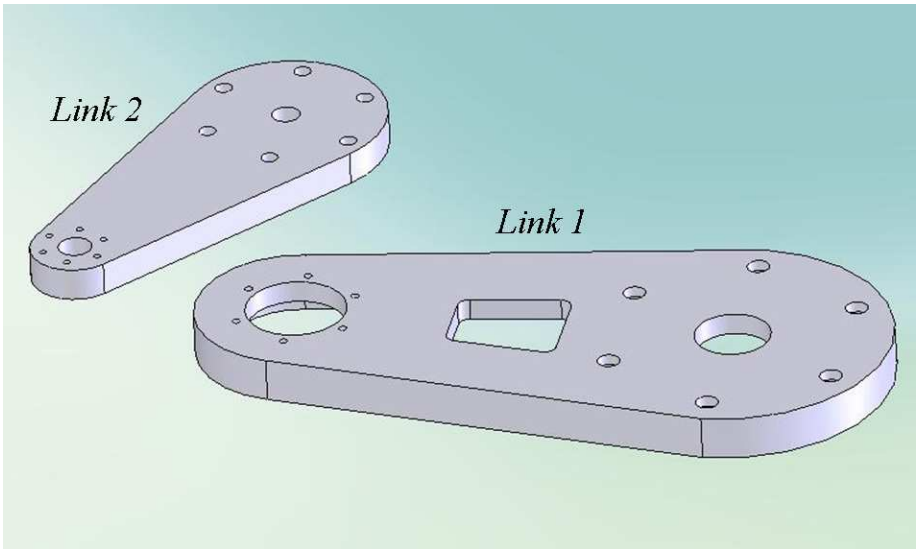

Figure 7.3 The direct drive SCARA type robot arm and link CAD models

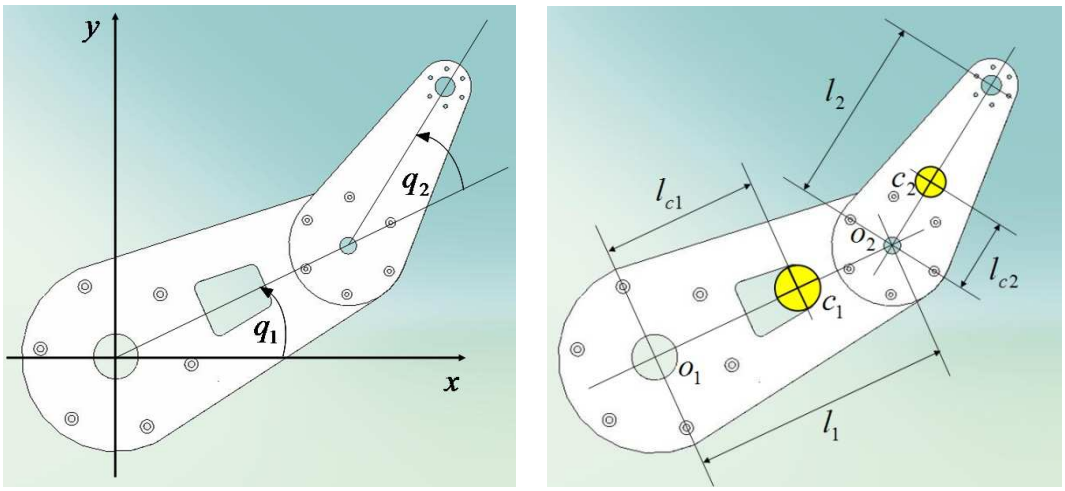

Fig. 7.4 Joint angle descriptions and length parameters of the direct drive SCARA type robot arm.

Table 7.1 Robot Dynamics Parameters

Link 1 weight (including elbow motor)	17.9 kg
Link 1 inertia (Including elbow motor)	0.54 kgm2
Motor 1 rotor inertia	0.167 kgm2
Link 1 length (Joint center to joint center)	0.4 m
Link 1 joint to center of mass distance	0.277 m
Joint 1 viscous friction coefficient	3 Nms/rad
Joint 1 Coulomb friction coefficient	4.5 Nm
Link 2 weight	3.25 kg
Link 2 inertia	0.04 kgm2
Motor 2 rotor inertia	0.019 kgm2
Link 2 length (Joint center to tool center)	0.28 m
Link 2 joint to center of mass distance	0.09 m
Joint 2 viscous friction coefficient	0.6 Nms/rad
Joint 2 Coulomb friction coefficient	1.1 Nm

7.2 Force Sensor System

An ATI Gamma type 6 axis industrial Force/torque sensor is assembled at the tip of link 2. The force sensor is via ATI CTL 9105 type Sensor controller box. The analog output of the controller box is connected to the analog input of dSPACE controller card. A M8 stud is mounted on top of the force sensor, concentric with it, and used as the tool in the experiments.

7.3 Vision System

The camera which overlooks the scene is a Philips SPC900NC series camera with resolution of 320x240 pixels and has a sampling rate of 30 fps. OpenCV library is used for

visual processing. Since dSPACE's compiler is not capable of compiling Open Computer Vision (OpenCV) Library, the visual processing routines are run in Visual Studio Environment, and data connection between servoing routine and visual processing routine is maintained by CLIB communication library of the dSPACE.

In experiments the vision system is used in this assignment for tracking the point of interest of the workpiece, detecting the orientation of the workpiece continuously and also for visual servoing purposes as explained in the previous chapters. The point on the workpiece is detected by feature detection algorithms and then tracked using optical flow based Lucas Kanade Feature Tracker [41]. The orientation of the workpiece is found using the following methods. First canny edge detection algorithm [42] is used. Among the edges found by this algorithm a Hough transform line detection algorithm is run. An implementation of this algorithm can be found in [43]. By this way the line on the workpiece is detected continuously and the slope of the detected line gives the orientation of the workpiece with respect to camera frame. The robot tool tip is again tracked by using Lucas Kanade Feature Tracker.

As it is stated in equation (6), task space errors e_V^x and e_V^y are used for visual servoing. These errors are calculated using trigonometry in image space. Figure 7.5 is presented for the explanation of this geometry.

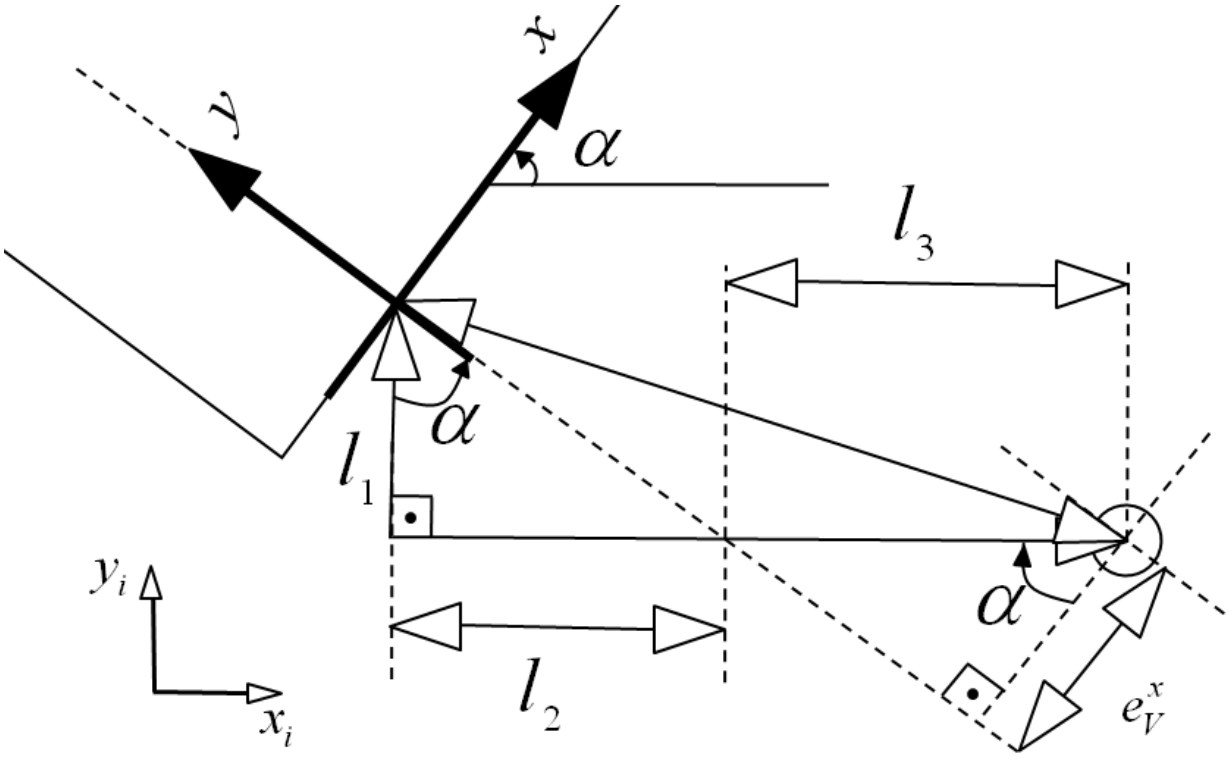

Figure 7.5 : Trigonametric Relations to Calculate Visual Servoing Errors.

In Figure 7.5, l_1 can be calculated by the difference between y coordinates of target point and tool tip point. This difference is denoted by Δy_i

$$\Delta y_i = l_1 \tag{7.1}$$

By multiplying the tangent of the task angle with l_1, l_2 can be computed.

$$l_2 = l_1 \tan(\alpha) \tag{7.2}$$

The summation of l_2 and l_3 is the difference between x coordinates target point and tool tip point. This difference is called Δx_i . Thus,

$$l_3 = \Delta x_i - l_2 \tag{7.3}$$

By multiplying l_3 with the cosine of the task angle e_V^x can be achieved.

$$e_V^x = l_3 \cos(\alpha) \tag{7.4}$$

Also, since the edge of the workpiece is detected, the equation of the this line is known. From this equation, the equation of the line that is perpendicular to the previous one, and that passes through the tool tip point can be obtained. The intersection point of these two lines is the closest point of tool tip to the workpiece, The length of the line segment equals to e_V^y, and can be calculated by applying Pythagorean theorem to the coordinates of the tool tip point and the intersection point.

7.4 Workpiece

The workpiece, a polymer sheet of 10 mm thickness with rectangular shape is pivoted around a vertical axis, and is free to rotate. Soft linear springs attached to the workpiece from both sides keep the orientation of it fixed when no external forces are applied on it.

7.5 Hierarchical Phase Template Algorithm

There are three implementations presented in this thesis. In all implementations Hierarchical Phase Template Algorithm is used. The task is divided into far away, near to, touching and manipulation phases. In far away phase, manipulator is servoed to the y-axis. When manipulator reaches to the y-axis, it moves along this axis towards the workpiece. When it comes to a certain with the workpiece, near to phase begins. In near to phase, the gain in y-axis direction is decreased. This slows down the manipulator, and a soft contact in order the achieve a soft contact with the workpiece.

A certain force threshold is set to detect the contact. Here, this threshold is specified as 0.5 Newton. As this threshold is measured by the force sensor, visual servoing in y-axis is turned off, and force control in this direction begins. The manipulation phase is different for each of three algorithms, and they are as explained in the previous sections. However the main aim of these algorithms is to apply certain amount.

7.6 Control Interface

A control interface is formed using dSPACE's interface tools. By the help of this interface, gains of the controllers are tuned, references to the controllers are given and the measurements are monitored. Also, the force application point is selected using this camera window of the dSPACE. A screenshot of the interface is in Fig.7.6.

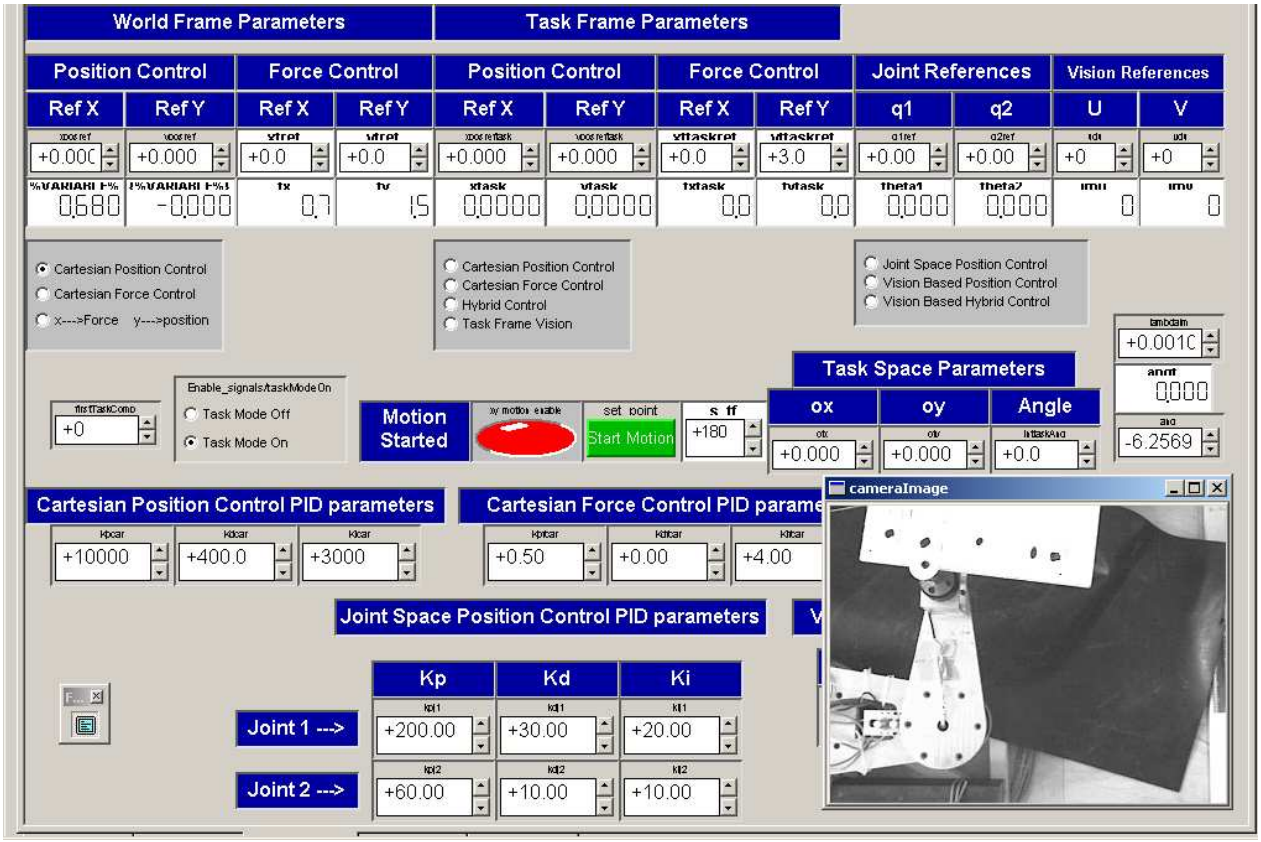

Figure 7.6 The interface

7.7 Experiments

The integrated visual/force control is tested i) in a hybrid approach without a fuzzy gain tuning (Chapter 4), ii) in a hybrid approach with a fuzzy gain tuning (Chapter 5), and iii) in a shared approach with fuzzy gain tuning (Chapter 6). The task frame orientation is identified with the angle α between the image frame and task frame x-axes in Fig. 7.3, and this angle is termed "task angle" in the text below.

7.7.1 Experimental Results of Fixed Parameter Hybrid Visual/Force Control

Experimental results with the first approach are presented in Fig. 7.7. This figure shows the task angle, the measured force in y-direction and y-direction position error in task space. At the beginning of the motion, manipulator quickly reduces the error in x-direction as

it can be seen in Fig. 7.7. c). In Fig. 7.7. b), around 13^{th} second a small peak is present. This is when touching phase begins, and visual servoing in y direction is turned off and force control in that direction starts. Approximately at 15^{th} second, force measurement converges to the force reference. As it can seen from Fig. 7.7 a) after force control reaches to steady state, the task angle is changed by manual intervention about 5 degrees. This motion introduces a position error in x and y-direction. In Fig. Fig. 7.7 b), it can be seen that, a hard impact occurs following the abrupt change in the task angle. After the impact, although there exists a nonzero position error in x-direction, the algorithm continues to apply force on the workpiece. As a result, an undesired shear force is observed and this force moves the workpiece further so that no force convergence is observed.

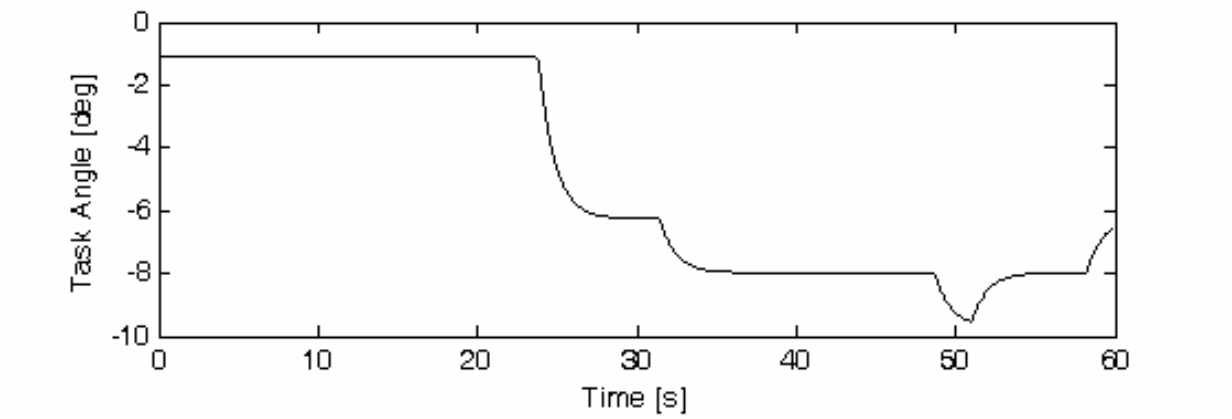

a)

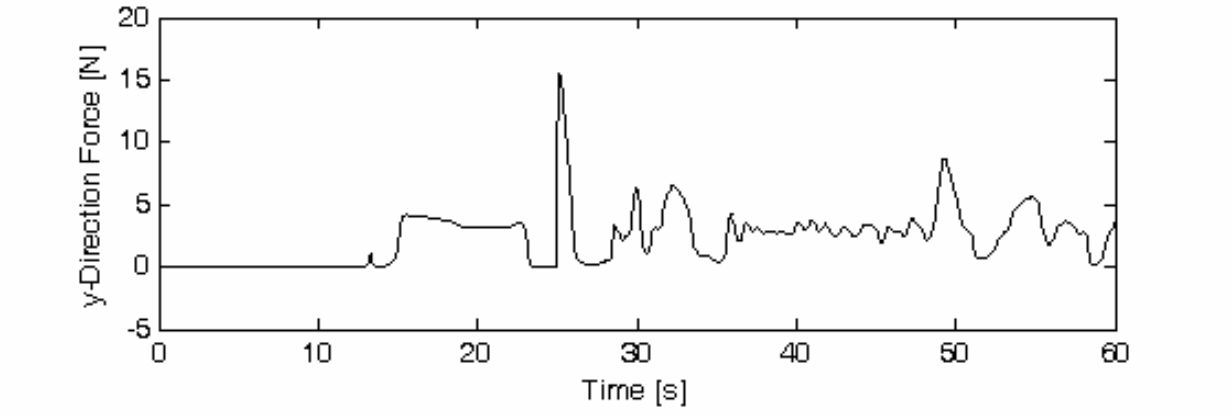

b)

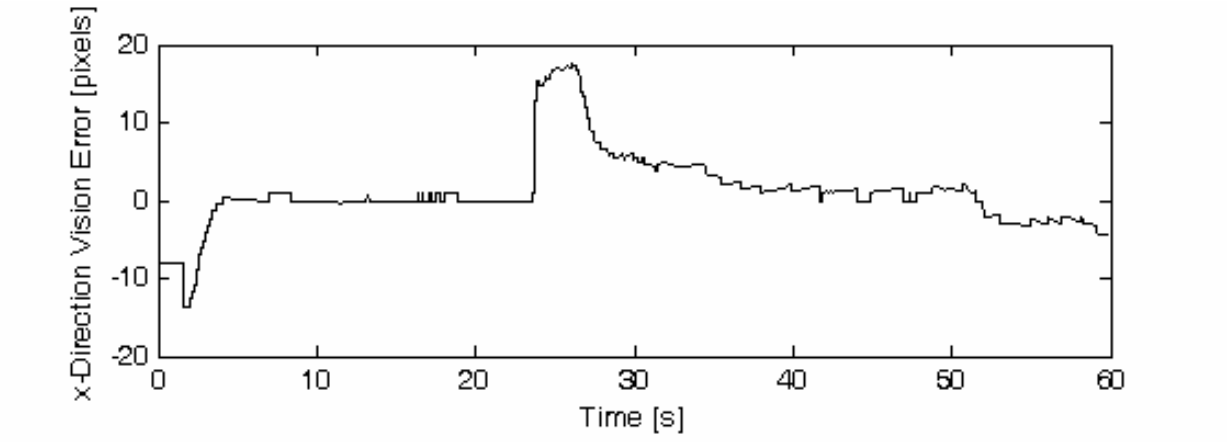

c)

Figure 7.7 Task angle, y-direction force, and x-direction visual servoing error without online fuzzy tuning

Controller gains that are used in this experiment are given in Table 7.2.

Table 7.2 Controller Parameters of Fixed Parameter Hybrid Visual/Force Control

K_V^y	0.4	K_{P_P}	10000
K_{p_F}	0.5	K_{I_P}	3000
K_F	7	K_{D_P}	400

7.7.2 Experimental Results of Hybrid Visual/Force Control with Fuzzy Parameter Tuning

The results obtained with the second approach are shown in Fig. 7.8. In this approach undesired sheer forces are overcome by fuzzy gain tuning. The motion before the manual motion of the workpiece is the same with the results of the previous section. With fuzzy tuning, when there appears a position error in x- direction, visual servoing gain in x-direction begins to climb where force control gain drops rapidly as in Fig. 7.8 a). This prevents the shear forces that are mentioned in the previous case. As the position error decreases to some specified degree which is defined by the fuzzy rule, force control gain rises. At this instance, however, if there is a position error in y-direction, the result is again a hard impact since only servoing in that direction is via force control. To stress the continuity of the performance of the algorithm, task angle is changed manually 2 times. The hard contact is observed in both task angles changes. However, after this impact, system comes to a steady state quickly.

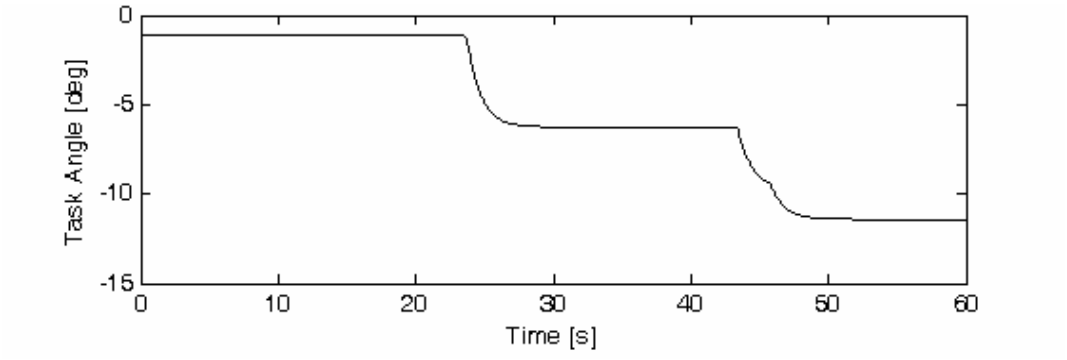

a)

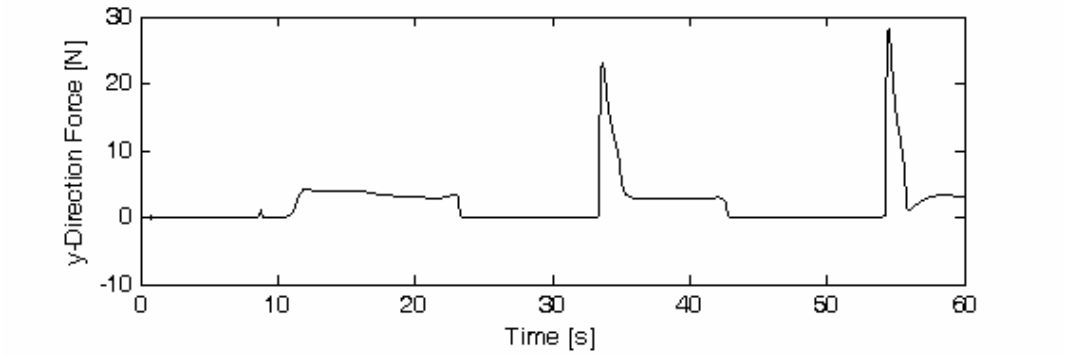

b)

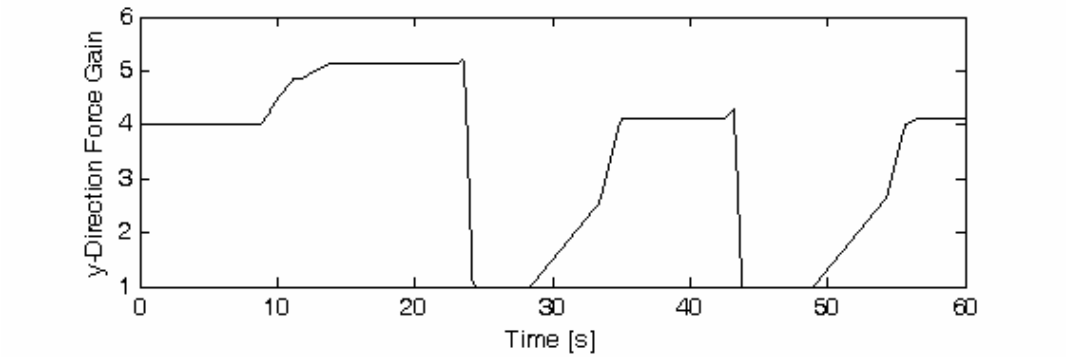

c)

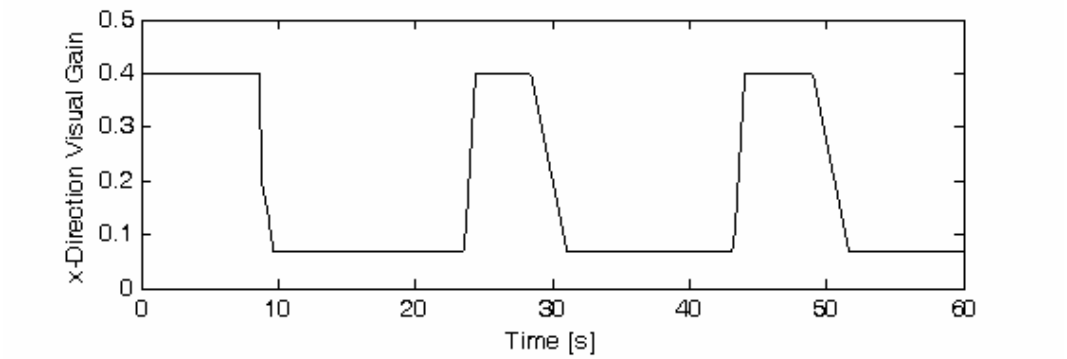

Figure 7.8 Task angle, y -direction force measurement and tuned gains using hybrid approach with fuzzy tuning

The fuzzy logic parameters that are used in this experiment is given in Table 7.3. Inner position loop parameters are the same with values in Table 7.2.

Table 7.3 Fuzzy Logic Parameters of Hybrid Visual/Force Control with Fuzzy Parameter Tuning

$\Delta K_{F^y PS}$	0.001	$e_{V^x S}$	1
$\Delta K_{F^y NB}$	-0.01	$e_{V^x B}$	5
$\Delta K_{F^y NS}$	-0.004	$e_{F^y S}$	0.2
$\Delta K_{V^x NS}$	-0.0004	$e_{F^y B}$	4
$\Delta K_{V^x PS}$	0.0004		
$\Delta K_{V^x NB}$	-0.0008		

7.7.3 Experimental Results of Shared Control with Fuzzy Parameter Tuning

To overcome the hard impact stated in the previous section of this chapter, the third method is applied and fuzzy logic tuned visual servoing is applied along the y-direction too along with the force control in manipulation phase. As it can be seen from Figure 7.9, and Figure7.10, when the workpiece starts to move, force gain rises to achieve continuous contact with the workpiece. This results with a rise in the applied force. However, since the contact is not broken yet, no hard impact is observed. A nonzero position error develops. Both of the visual servoing gains (x and y-direction) are increased in order to get close to the target point and the force gain is reduced since the desired force application point is positioned far from the tool. The robot tool tip gets close to the workpiece, and touches it with visual servoing in y-direction. The gain of visual servoing in y-direction is not decreased unless some amount of force is measured. This is like a feedforward effect for force control. Meanwhile, since the position error in y-direction is reduced, force control gain starts to increase.

As the amount of applied force increases to some degree which is specified by fuzzy membership functions, visual servoing gain in y-direction is decreased and the force exertion task is left to force controller. During this exchange an overshoot in the force is observed.

However, it is much less pronounced then with the previous method in which a hard impact was observed.

By using this method, the application of Hierarchical Phase-Template Algorithm becomes redundant. Since this algorithm turns force control off when the position error is too big. Thus it can also be used when the manipulator is far away from the workpiece.This is another important advantage of the proposed algorithm.

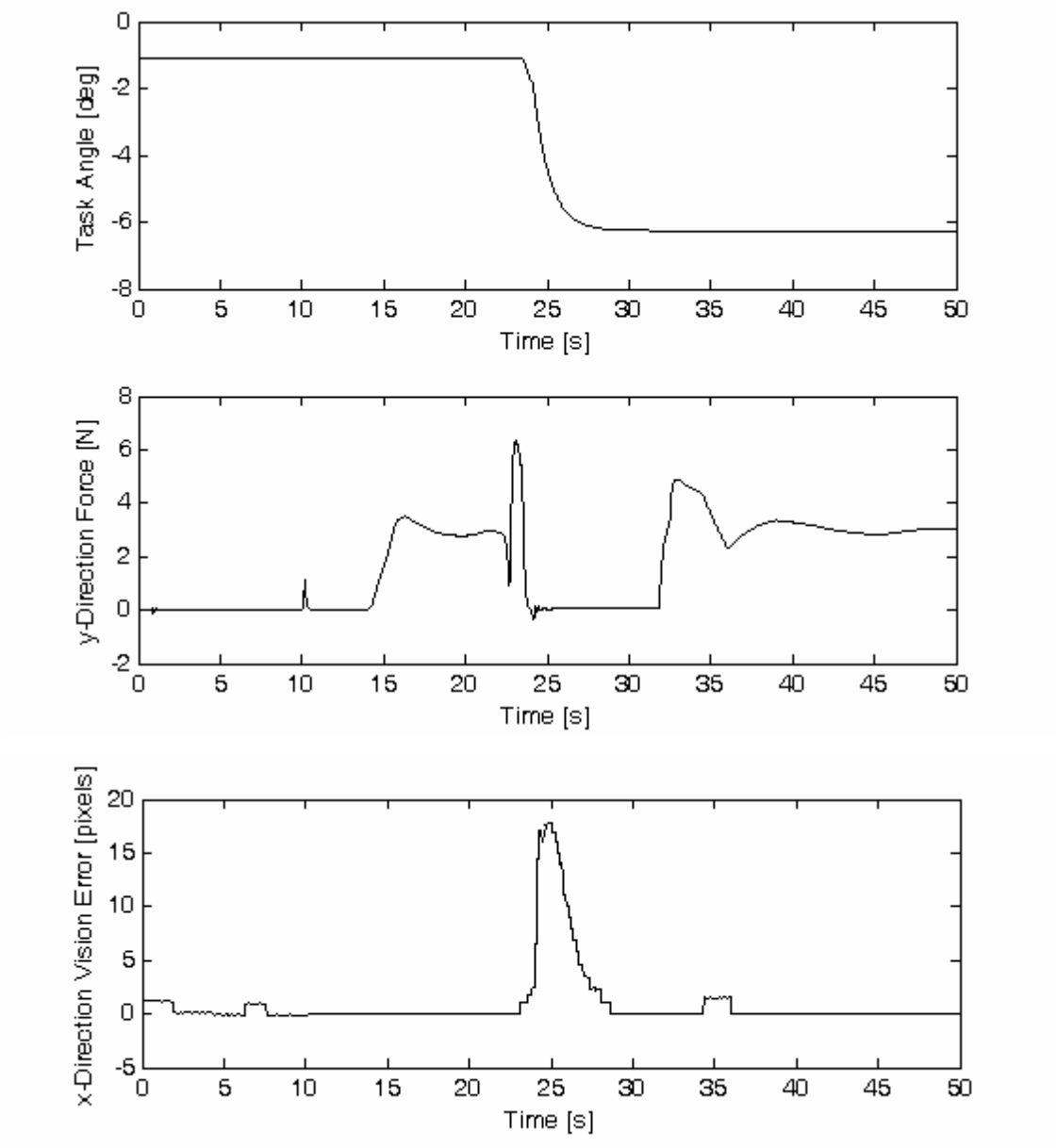

Figure 7.9 Task angle, y-direction force, and x-direction visual servoing error

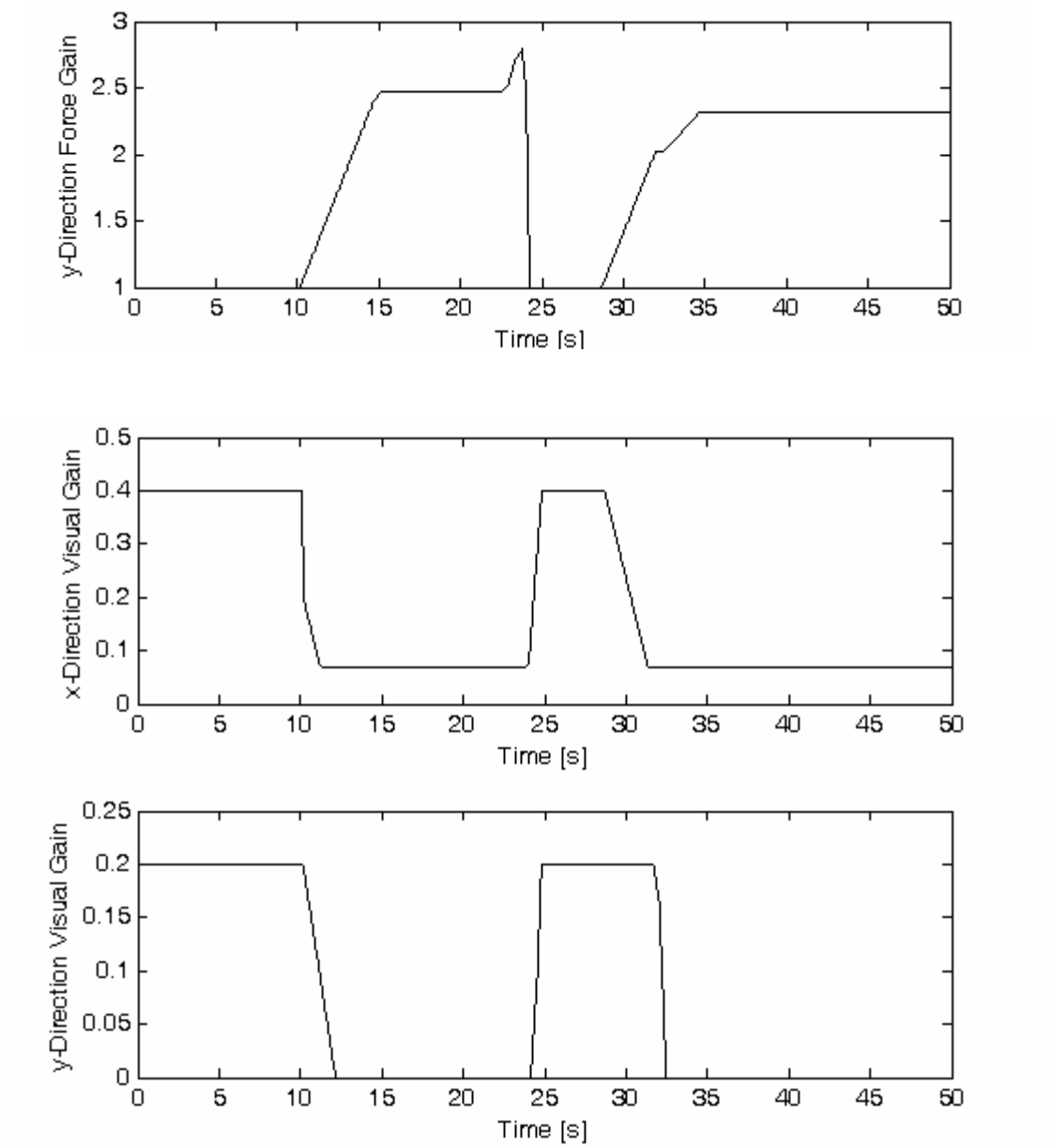

Figure 7.10 The tuned Visual Servoing and Force Control Gains in Shared Approach

Fuzzy logic parameters are used with the values in Table 7.4

Table 7.4 Fuzzy Logic Parameters of Shared Control with Fuzzy Parameter Tuning

$\Delta K_{F^y PS}$	0.001	$e_{V^x S}$	1
$\Delta K_{F^y NB}$	-0.01	$e_{V^x B}$	4
$\Delta K_{F^y NS}$	-0.004	$e_{F^y S}$	0.5
$\Delta K_{V^x NS}$	-0.0004	$e_{F^y B}$	1.5
$\Delta K_{V^x PS}$	0.0004	$\Delta K_{V^x NB}$	-0.0008
$\Delta K_{V^y NS}$	-0.0001	$\Delta K_{V^y PS}$	0.0001
$\Delta K_{V^y NB}$	-0.0004	$\Delta K_{V^y PB}$	0.0004

Chapter 8

8. CONCLUSION

In this thesis, a hybrid vision/force control approach with fuzzy logic tuned controller gains is proposed. The method is then further improved by making the original force controlled direction a shared one by adding a fuzzy logic tuned visual servoing along this direction. The method is tested on a direct drive robot. It is seen that, with online fuzzy tuning, the system avoids hard impacts and sheer forces. These effects are not only undesirable because of the task definition, but also possible reasons for instability. Thus, preventing these effects is significant and the proposed algorithms, especially the shared one, achieves it. The fuzzy tuned approaches are novel. The first application of fuzzy tuning to a vision/force integration problem is with the presented work. The results show that fuzzy logic can be very useful in this kind of integration.

Also the fuzzy parameter tuned shared algorithm removes the necessity to divide the task into phases. Most of the algorithms in literature, use a structure like the hierarchical phase template and divide tasks into phases like far-away, near to, touching and manipulation. They assign different controllers to different phases. The fuzzy-shared algorithm proposed in this thesis does not need this kind of switching and works in all the phases of the task.

As it can be seen from the literature survey, there are various different visual servoing and force controllers in literature. The combination of different controllers can be tried with the above proposed gain tuning approach to improve the performance of the control system.

REFERENCES

[1] R. Bolles and R. Paul, The use of Sensory feedback in a Programmable Assembly System: *Stanford Artificial Intelligence Laboratory*, MEMO AIM-220, STAN-Cs-396, Oct. 1970.

[2] Feddema J. T., Mitchell O. R., "Vision-Guided Servoing with Feature-Based Trajectory Generation", *IEEE Transaction on Robotics and Automation*, Vol. 5, No. 5, October 1989.

[3] S. Hutchinson, G.D. Hager and P. Corke, "A Tutorial Introduction to Visual Servo Control," *IEEE Transactions on Robotics and Automation*, Vol. 12, No. 5, pp. 651-670, 1996.

[4] Corke P. I., "Visual Control of Robots, High Performance Visual Servoing", *Research Studies Press,* 1996.

[5] Deguchi K. "Optimal Motion Control for Image-Based Visual Servoing by Decoupling Translation and Rotation" *Proceedings of the IEEE/RSJ International Conference on Intelligent Robots and Systems*, October 1998.

[6] Hashimato K., Kimoto T., Ebine T., Kimura H., "Manipulator Control with Image-Based Visual Servo", *Proceedings of the IEEE International Conference on Robotics and Automation,* April 1991

[7] Wilson W. J., Hulls C. C. W., Bell G. S., "Relative End-Effector Control Using Cartesian Position Based Visual Servoing", IEEE Transactions of robotics and Automation, Vol. 12, No. 5, October 1996.

[8] Martinet P., Gallice J., "Position based visual servoing using a non-linear approach", Proceedings of the *IEEE/RSJ, International Conference on Intelligent Robots and Systems, 1999.*

[9] Malis E., Chaumette F., "2 1/2 D Visual Servoing with Respect to Unknown Objects Through a New Estimation Scheme of Camera Displacement", *International Journal of Computer Vision,* 37(1), 79–97, 2000.

[10] Gans N. R., Hutchinson S. A., "An Experimental Study of Hybrid Switched System Approaches to Visual Servoing", *Proceedings of IEEE International Conference of robotics and Automation,* 2003.

[11] Kim J. K., Kim D. W., Choi S.J., Won S. C. "Image-based Visual Servoing using Sliding mode control" *SICE-ICASE International Joint Conference*, 2006.

[12] Parra-Vega, V., Fierro-Rojas J. D., Espinosa-Romero A., "Uncalibrated Sliding Mode Visual Servoing of Uncertain Robot Manipulators", *Proceedings of the IEEE/RSJ, International Conference on Intelligent Robots and Systems,* 2002.

[13] Astolfi A., Hsu L., Netto M.S., Ortega R., " Two solutions to the adaptive visual servoing problem", IEEE Transactions on Robotics and Automation, Vol.18, 387-392, June 2002.

[14] Perra-Vega V., Fierro-Rojas J. D., Espinosa-Romero A., "Adaptive Sliding Mode Uncalibrated Visual Servoing for Finite-time Tracking of 2D Robot" *Proceedings of the IEEE l International Conference on Robotics & Automation,* September 2003.

[15] P. Jiang, R. Unbehauen, "Robot Visual Servoing With Iterative Learning Control", *IEEE Transactions on Systems, Man, and Cybernetics,* Vol. 32, No.2, March 2002.

[16] Zeng G. and Hemami A.,"An overview of robot force control", *Robotica*, Vol. 15, pp. 473-482, 1997.

[17] Salisbury, J.K., "Active Stiffness Control of a Manipulator in Cartesian Coordinates" *Proceedings of IEEE Conference on Decision and Control,* 1980.

[18] Hogan N., "Impedance Control: An Approach to Manipulation", *Journal of Dynamic Systems, Measurement, and Control*, Vol. 107, 1-24, March 1985.

[19] Dégoulange E., Dauchez P., "External force control of an industrial puma 560 robot", *Journal of Robotic Systems,* Vol. 11, No. 6, pp. 532-540, 1994.

[20] H . Seraji , ‘‘Adaptive Admittance Control : An Approach to Explicit Force Control in Compliant Motion’’, *IEEE International Conference on Robotics and Automation* pp . 2705-2712 , 1994.

[21] M. Mason, "Compliance and Force Control for Computer-Controlled Manipulators," *IEEE Trans on Systems, Man, and Cybernetics,* Vol. 11, No. 6, pp. 418—432, 1981.

[22] Khatib O ., ‘‘A Unified Approach for Motion and Force Control of Robot Manipulators : The Operational Space Formulation’’, *IEEE Journal of Robotics and Automation,* RA-3 (1) , 43-53, 1987 .

[23] Raibert M . H., Craig J . J., ‘‘Hybrid Position / Force Control of Manipulators’’ ASME *Journal of Dynamic Systems, Measurement, and Control,* Vol.102 , pp. 126-133, 1981 .

[24] Cai L., Goldenberg A. A., ‘‘An Approach to Force and Position Control of Robot Manipulators’’ IEEE International Conference on Control and Application, pp. 86-90, 1989.

[25] Anderson R. J., Spong M. W., “Hybrid Impedance Control of Robotic Manipulators”, *IEEE Journal of Robotics and Automation*, Vol.4 No.5 1988.

[26] Eppinger S. D., Seering W. P., “Understanding Bandwidth Limitations in Robot Force Control”, *IEEE Proceedings of the International Conference on Robotics and Automation,* April 1987.

[27] Volpe R., Khosla P., “An Experimental Evaluation and Comparison of Explicit Force Control Strategies for Robotic Manipulators”, *Proceedings of the IEEE International Conference of Robotics and Automation,* pp.1387-1393, May 1992.

[28] Yabuta T., Yamada T., Tsujimura T, Sakata H., “Force Control of Servomechanism Using Adaptive Control”, IEEE International Journal of Robotics and Automation, Vol.4 No.2, pp.223-238 April 1988.

[29] J . J . Craig , ‘‘Adaptive Control of Manipulators through Repeated Trails’’, *American Control Conference*, pp. 1566-1573, 1984.

[30] Slotine J. E., "Sliding controller design for non-linear systems", *International Journal of Control,* Vol. 40, I. 2, pages 421 – 434, August 1984.

[31] Jeon D., Tomizuka M., "Learning Hybrid Force and Position Control of Robot Manipulators", *IEEE Transactions on Robotics and Automation*, Vol. 9, No. 4, August 1993.

[32] S . R . Pandian and S . Kawamura , ''Hybrid force / position control for robot manipulators based on a D-type learning law", *Robotica* , Vol. 14 , Part I , pp. 51-59, 1996.

[33] Luo R. C., Kay M. G., "Multisensor Integration and Fusion in Intelligent Systems", *IEEE Transactions on Systems, Man, and Cybernetics* Vol. 19, No. 5 1989.

[34] Nelson B. J., Morrow J. D., Khosla P. K., "Robotic Manipulation Using High Bandwidth Force and Vision Feedback", *International Journal of Mathematical and Computer Modelling*, pp. 1-29, 1995.

[35] Baeten J., Schutter J. D., "Integrated Visual Servoing and Force Control, the Task Frame Approach", *Springer tracts in advanced robotics,* Heidelberg, 2004.

[36] Morel G., Malis E., Boudet S., "Impedance based coimbination of visual and force control", *Proceedings of the IEEE International Conference on Robotics & Automation,* May 1998.

[37] Zadeh L.A., "Fuzzy sets" *Information and control*, 8(3), pp.338-353, 1965.

[38] Zadeh, L. A., "Fuzzy Logic = Computing with Words", *IEEE International Transactions on Fuzzy Systems,* Vol. 4, No. 2, May 1996.

[39] Palm R., "Robust Control by Fuzzy Sliding Mode", *Automatica*, Vol. 30, pp. 1429-1437, 1994.

[40] Erbatur, K. Calli, B., "Fuzzy Boundary Layer Tuning as Applied to the Control of a Direct Drive Robot", IECON, pp. 2858-2863, 2007.

[41] Bouguet J., "Pyramidal Implementation of the Lucas Kanade Feature Tracker Description of the Algorithm*." Intel Corporation, Microprocessor Research Labs*, OpenCV Documents, 2000.

[42] Canny, J. F. “A computational approach to edge detection”, *IEEE Transactions on Pattern Analysis & Machine Intelligence,* Vol. 8, No.6, pp. 679-698, 1986.

[43] Yuen H.K., Illingworth J. and Kittler J., “Detecting partially occluded ellipses using the Hough transform” *Image and Vision Comput.* Vol. 7, No. 1, pp. 31-37, 1989.